

Critical Josephson current in BCS-BEC crossover superfluids

M. Zaccanti^{1,2} and W. Zwerger³

¹*Istituto Nazionale di Ottica del Consiglio Nazionale delle Ricerche (INO-CNR), 50019 Sesto Fiorentino, Italy*

²*LENS and Dipartimento di Fisica e Astronomia, Università di Firenze, 50019 Sesto Fiorentino, Italy*

³*Physik-Department, Technische Universität München, D-85748 Garching, Germany*

We develop a microscopic model to describe the Josephson dynamics between two superfluid reservoirs of ultracold fermionic atoms which accounts for the dependence of the critical current on both the barrier height and the interaction strength along the crossover from BCS to BEC. Building on a previous study [F. Meier & W. Zwerger, *Phys. Rev. A*, **64** 033610 (2001)] of weakly-interacting bosons, we derive analytic results for the Josephson critical current at zero temperature for homogeneous and trapped systems at arbitrary coupling. The critical current exhibits a maximum near the unitarity limit which arises from the competition between the increasing condensate fraction and a decrease of the chemical potential along the evolution from the BCS to the BEC limit. Our results agree quantitatively with numerical simulations and recent experimental data.

I. INTRODUCTION

Josephson weak links [1, 2] represent a paradigmatic tool to investigate phase coherence between coupled superfluids [3, 4], and they have been realized in a variety of different setups: From solid state systems [5], where the Josephson effect has played a crucial role, e.g. to unveil the d -wave nature of pairing in high temperature superconductors [6, 7], to neutral superfluids of liquid Helium [8, 9] and weakly interacting Bose condensates of ultracold atoms [10–21]. More recently, both theoretical [22–26] and experimental [27–30] efforts have been targeted to investigate the Josephson dynamics in the context of ultracold superfluids of strongly interacting fermion pairs. The so-called BCS-BEC crossover [31, 32] which relies on exploiting Feshbach resonances between two different hyperfine states of ultracold fermions [33], offers the unique possibility to investigate, within a single physical system, Josephson tunneling from the standard BCS limit of weakly bound fermion pairs to a Bose Einstein condensate of tightly bound molecules, including the scale invariant unitary Fermi gas at infinite scattering length as an intermediate phase.

In contrast with their bosonic counterparts, crossover superfluids are a challenging system to explore. On the experimental side, the strong interactions require, for coherent Josephson dynamics to be unveiled, the imprinting of thin barrier potentials on the sample, with thicknesses on the order of very few interparticle spacings [29, 30]. On the theoretical side, the crossover regime poses a difficult many-body problem for which many observables are accessible only by approximate methods [32]. In particular, microscopic calculations of the Josephson currents based on the solution of Bogoliubov de Gennes equations (BdGE) have been reported in Refs. [22, 25, 26]. Although they provide a qualitatively correct description of the entire crossover region, the approach is quantitatively reliable only in the BCS limit. An alternative strategy relies on the zero-temperature extended Thomas-Fermi models (ETFM) [23, 24, 26]. These approaches are based on a generalized Gross-Pitaevskii equation for

the complex order parameter $\psi(\mathbf{r})$ of bosonic pairs with mass $M = 2m$ which tunnel across a barrier of effective height $V_0 = 2V_{0f}$. Here m and V_{0f} denote the mass and barrier height of a single fermion. The pair density is linked to the total fermion density $n = n_\uparrow + n_\downarrow$ by $|\psi(\mathbf{r})|^2 = n(\mathbf{r})/2$ (for more details, see e.g. Ref. [26]). A key ingredient of the EFTM non-linear equation is the local chemical potential of pairs μ_B which is related to the chemical potential $\mu(n, a)$ of a uniform Fermi gas with total density n and interspecies scattering length a by $\mu_B(n, a) = 2\mu(n, a) + |\epsilon_b| \equiv 2\mu_F(n, a)$. Here, ϵ_b is the binding energy of one dimer in the vacuum ($\epsilon_b = 0$ for $a < 0$). The advantage of this framework, compared with the mean field BdGE approach, is that $\mu(n, a)$ is an independent, purely thermodynamic input parameter for the calculation of the Josephson current. Hence, the correct chemical potential throughout the crossover can be accounted for by including the corresponding results obtained from independent Quantum Monte-Carlo calculations, see e.g. Ref. [34]. Nonetheless, it turns out that the EFTM method can properly describe the Josephson effect only in the BEC limit but it fails, even qualitatively, in the unitary and BCS regimes [26, 29]. In particular, for fixed barrier heights, EFTM calculations yield a monotonically increasing Josephson current when moving from the BEC to the BCS limit. By contrast, the critical current is found to reach a maximum value near unitarity both experimentally [29, 30] and also in the numerical BdGE calculations [22, 25, 26]. Therefore, developing a unified model which provides a quantitatively correct description of the Josephson effect throughout the BCS-BEC crossover represents a relevant and timely problem, which is addressed in the present study.

Our work builds upon a previous microscopic description of the Josephson dynamics between two weakly interacting Bose Einstein condensates by one of us [12]. We will show that a straightforward extension of this model to fermionic superfluids quantitatively reproduces both the results of numerical simulations and also the experimental data over a wide range of parameters. Surprisingly, this holds even beyond the weak tunneling limit considered in the underlying microscopic model. Our

study suggests that, throughout the BCS-BEC crossover, the critical Josephson current can be evaluated analytically solely on the basis of (i) the single-particle transmission amplitude for a pair at the relevant chemical potential, and (ii) bulk properties of the superfluid at equilibrium, specifically, the condensate density and the pair chemical potential. Most importantly, our approach provides a straightforward explanation for the experimentally observed maximum of the critical current density near unitarity which arises from two competing effects: the increase of the condensate fraction and the concurrent decrease of the chemical potential as a function of the dimensionless coupling strength $1/k_F a$. The identification of the unitary gas as the most stable fermionic superfluid [22, 35–38] thus appears from a viewpoint which applies uniformly over the whole regime from weak to strong coupling, with no need to invoke different dissipation mechanisms, such as pair breaking on the BCS and phonon-like excitations on the BEC side [22, 26, 35].

II. JOSEPHSON CURRENT FROM BCS TO BEC

In the following, we will argue that the results obtained in Ref. [12] for the Josephson current between two weakly interacting BEC's can be extended in a straightforward manner to fermionic superfluids. This will provide an analytical result which holds throughout the full crossover from BCS to BEC. We start by considering a generic setup of a Josephson junction with the geometry depicted in Fig. 1a, where a rectangular barrier connects two homogeneous reservoirs. The results obtained for this idealized case will then be generalized to the harmonically trapped situation and Gaussian barriers sketched in Fig. 1b, relevant to compare our model predictions with experimental data [29, 30].

For barrier heights V_0 which considerably exceed the boson chemical potential μ_B , it has been shown in Ref. [12] that the Josephson currents can be evaluated analytically in a systematic expansion in powers of an effective transfer Hamiltonian \hat{H}_T . In leading order, this gives rise to a non-dissipative Josephson current between the two superfluid reservoirs with a sinusoidal current-phase relation $I(\varphi) = I_c \sin \varphi$, where φ is the difference between the condensate phases across the junction [39]. Assuming a homogeneous situation with transverse area $A = L^2$, the associated critical current density

$$\hbar j_c = \frac{\hbar I_c}{A} = 2B t_{cc}(\mu_B) n_c \quad (1)$$

can be expressed as the product of the transfer matrix element $t_{cc}(\mu_B)$, associated with coherent tunneling of bosons at an energy equal to their equilibrium chemical potential μ_B , times the associated condensate density n_c . Formally, Eq. (1) also contains the total longitudinal size $2B$ of the system which however drops out, as expected. Indeed, for the junction geometry of Fig. 1a, the matrix

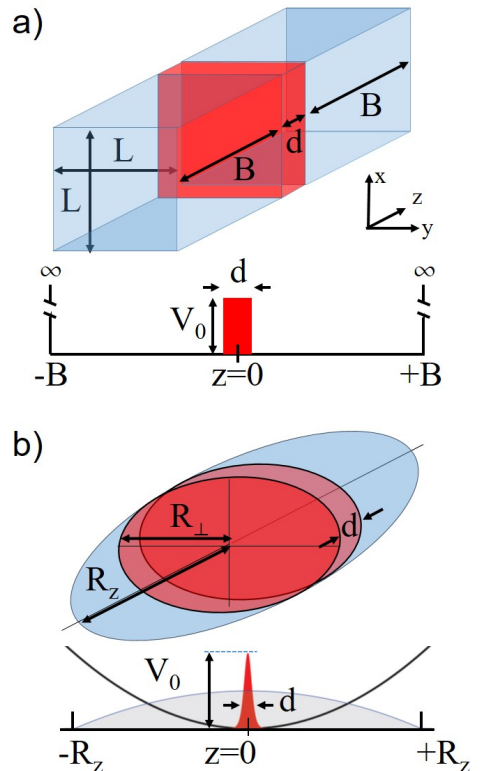


FIG. 1. Sketch of the Josephson junction setups considered in this work. a) Model geometry relevant for Refs. [12, 26], where a rectangular barrier separates two symmetric homogeneous reservoirs. b) Geometry of the Josephson junction experimentally investigated in Refs. [29, 30] where a Gaussian barrier bisects a superfluid confined within a harmonic potential. The radial R_{\perp} and axial R_z radii, set the effective section and longitudinal size of the two reservoirs, respectively.

element t_{cc} has been evaluated in Ref. [12], and it can be conveniently recast as

$$t_{cc}(\mu_B) = \frac{|t|(\mu_B)}{4k(\mu_B)B} \mu_B. \quad (2)$$

Here $k(\mu_B) = \sqrt{2M\mu_B}/\hbar$ is the wave vector of a boson with mass M and chemical potential μ_B , while $|t|(\mu_B)$ is the associated single-particle transmission amplitude. The critical current density can be therefore expressed in the simple form

$$\hbar j_c = \frac{\mu_B n_c}{2k(\mu_B)} |t|(\mu_B) \quad (3)$$

which shows that inter-particle interactions affect j_c only through bulk properties of the superfluid. Specifically, they involve the chemical potential μ_B and the condensate density n_c which, to lowest order in the interactions between the pairs, coincides with the full Bose density. It is important to notice that the microscopic tunneling amplitude $|t|(\mu_B)$ is the one for a *single* boson. It depends on the interaction strength only to the extent that this

determines the relevant energy at which the tunneling process occurs. As discussed in Ref. [12], the separation between single particle and many-body properties within Eq. (3) originates from the underlying assumption that the barrier height V_0 greatly exceeds the chemical potential μ_B . Under these conditions, our major claim in the following is that Eq. (3) correctly describes the Josephson current at *any* coupling strength.

The fact that Eq. (3) may hold even for fermionic superfluids throughout the crossover from the BCS to the BEC limit is supported by the quite remarkable observation that, upon a proper identification of the variables, this result essentially coincides with the well known expression for the critical current between two BCS superconductors. Within BCS theory, the critical current of a Josephson junction in the tunneling limit is known to be equal to the current flowing in the normal state at a finite applied voltage $eV = \pi\Delta_0/2$, where Δ_0 is the energy gap at zero temperature [1, 3, 40]. By evaluating the normal state conductance per unit area, which scales linearly with the number of discrete transverse modes, the Ambegaokar-Baratoff (AB) formula for the *pair* current density between two BCS superfluids coupled by a thin tunneling barrier can be expressed in the form [25]

$$\hbar j_c^{AB} = \frac{\pi}{2} \Delta_0 \frac{k_F^2}{16\pi^2} |t|^2(\mu_F) \quad (4)$$

where $|t|^2(\mu_F)$ is the transmission probability of a single fermion at the Fermi energy $\mu_F \rightarrow \epsilon_F$. While at a first glance the expressions in Eqs. (3) and (4) appear totally disconnected, it turns out that they are essentially equivalent. Indeed, in the BCS limit, the condensate density $n_c = \lambda_0 \cdot n/2$ is linked to the gap by the relation (see e.g. Refs. [41, 42])

$$\lambda_0^{\text{BCS}} = \frac{3\pi}{8} \frac{\Delta_0}{\epsilon_F} \quad (5)$$

where $n = k_F^3/(3\pi^2)$ is the total fermion density and λ_0 denotes the condensate fraction. Hence, Eq. (4) can be recast in the form

$$\hbar j_c^{AB} = \frac{\mu_F n_c}{2k_F} |t|^2(\mu_F) \quad (6)$$

where the similarity with Eq. (3) is now apparent. Indeed, noting that $2k_F \sim 2\sqrt{2m\mu_F}/\hbar \rightarrow k(\mu_B)$ in terms of the chemical potential $\mu_B = 2\mu_F$ of pairs, the two expressions are perfectly equivalent if the transmission probability $|t|^2(\mu_F)$ of a single Fermion is replaced by the transmission amplitude $|t(\mu_B)$ of a pair.

More specifically, it is instructive to consider the thermodynamic prefactor, common to the BCS result Eq. (6) and the BEC one Eq. (3) for the critical current density, for a fermionic superfluid at arbitrary coupling. This quantity, which encodes the many-body properties of the system, can be suitably expressed in terms of the condensate fraction $\lambda_0 = 2n_c/n$ and the dimensionless chemical potential $\tilde{\mu} = \mu_F/\epsilon_F$ of one fermion, which enters into

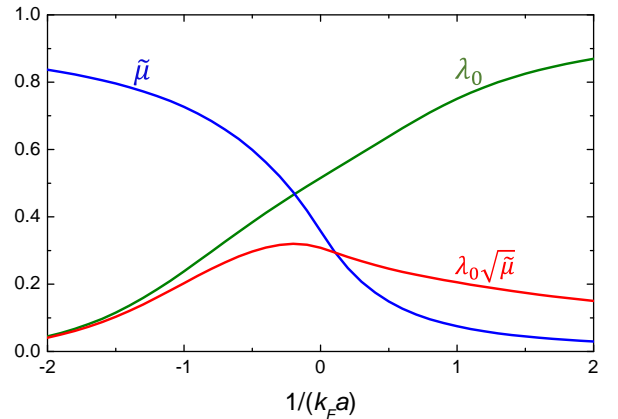


FIG. 2. Condensate fraction λ_0 (green line) and normalized chemical potential $\tilde{\mu} = \mu_F/\epsilon_F$ (blue line) obtained within a Luttinger-Ward approach at zero temperature [43], as a function of the dimensionless coupling strength $1/k_F a$. The product $\lambda_0 \sqrt{\tilde{\mu}}$ (red line), which determines the dependence of the critical Josephson current on interactions according to Eq. (7), exhibits a maximum near unitarity.

the BEC result Eq. (3) through the standard mapping $\mu_B(n, a) = 2\mu(n, a) + |\epsilon_b| \equiv 2\mu_F(n, a)$ between the Bose and Fermi chemical potential discussed in the previous section. With $v_F = \sqrt{2\epsilon_F/m}$ as the Fermi velocity of the non-interacting Fermi gas one obtains

$$\frac{j_c}{|t(\mu_B)|} = \frac{j_c^{AB}}{|t|^2(\mu_F)} = \frac{nv_F}{8} \lambda_0 \sqrt{\tilde{\mu}}. \quad (7)$$

Eq. (7) shows that the critical current density, in units of the natural scale set by (nv_F) , is determined by the product of the condensate fraction λ_0 with the square root of the (normalized) fermion chemical potential $\sqrt{\tilde{\mu}}$. The dependence of these two thermodynamic quantities on the coupling strength is shown in Fig. 2, which presents the results for λ_0 (green line) and $\tilde{\mu}$ (blue line) obtained within a Luttinger-Ward approach to the BCS-BEC crossover problem developed by Haussmann *et al.* [43]. Apparently, these two bulk properties exhibit an opposite behavior as a function of the coupling strength: while $\tilde{\mu}$ monotonically decreases from one towards zero upon moving from the BCS to the BEC limit, the condensate fraction λ_0 monotonically increases from exponentially small values in the BCS regime towards unity for a weakly interacting Bose superfluid. A qualitatively similar behavior is also obtained within a mean field BdGE approach, see e.g. Ref. [44] and references therein. However, the results of the two theories differ substantially on a quantitative level. In particular, for the gas at unitarity, mean field calculations yield a condensate fraction $\lambda_0 \sim 0.7$ instead of 0.51, and a chemical potential $\tilde{\mu} \sim 0.56$ instead of the value 0.36 obtained within the Luttinger-Ward approach, which agrees quite well with the experimental value $\tilde{\mu} = \xi_s = 0.37$ for the associated Bertsch parameter, see [45]. As a consequence of the

competing trends of λ_0 and $\tilde{\mu}$, the thermodynamic prefactor in Eq. (7) reaches a maximum near unitarity (see red line in Fig. 2), in qualitative agreement with both experimental [29] and numerical [22, 26] findings. Note, however, that the origin of the non-monotonic behavior in the present theory is quite different from the interpretation given by Spuntarelli *et al.* [22] for the case of weak barriers. There, following a Landau criterion, the rise and fall of the maximum Josephson current was ascribed to the existence of two distinct types of critical velocities associated with two different excitation branches: pair-breaking on the BCS and phonons on the BEC side, respectively. By contrast, our result Eq. (7) shows that in the tunneling regime this peculiar non-monotonicity emerges from the competition between λ_0 and $\tilde{\mu}$ uniformly throughout the crossover region. This conclusion is further supported by recent experimental studies [29, 30], which unambiguously identified vortex rings and phonons, rather than "fermionic" pair-breaking excitations, as the microscopic mechanisms responsible for the breakdown of the dissipationless flow, even on the BCS side of the crossover.

In the following, we focus on the difference between the BEC result in Eq. (3) and the BCS one of Eq. (6) that, as highlighted in Eq. (7), amounts to the ratio between the tunneling amplitude of one pair and the transmission probability of one fermion, evaluated at their relevant energies. Naively, such a quantity could be expected to exhibit an exponential dependence upon the barrier thickness d and the normalized height V_0/μ_B , hence causing a large quantitative mismatch between the BCS and BEC results. However, employing the mapping of the "fermionic" BdGE approach onto the "bosonic" EFTM one [26], it can be verified that this is not the case: The ratio of these two transmission terms is of order unity for a wide range of barrier geometries, featuring only a very weak dependence upon the barrier properties and the chemical potential. Indeed, applying Eq. (3) to the BCS limit of the crossover yields a critical current density that matches the BCS result Eq. (6) within a few 10% accuracy. For instance, over an extremely wide range $k_F d \in [10^{-3}, 10^2]$ of dimensionless barrier thicknesses, the two terms match one another within $\pm 50\%$, both for rectangular and Eckart barriers of relative heights $V_0/\mu_B \in [1, 10^4]$. Within the experimentally relevant regime of barrier widths $1 \lesssim k_F d \lesssim 4$ and moderate heights, $V_0/\mu_B \lesssim 2$ [29, 30], the deviations are in fact smaller than 20%. In view of these results, in the following we will thus use the extension of the bosonic expression Eq. (3) to arbitrary couplings to describe the critical current of a Josephson junction along the entire BCS-BEC crossover.

In order to benchmark our analytic theory against numerical and experimental results, it is necessary to also take into account higher harmonics that contribute to the critical current. In fact, as already mentioned in the previous section, the tunneling limit of exponentially small values of $|t|(\mu_B)$ is hard to achieve in practice and realis-

tic barrier heights V_0 are close to, or only slightly larger than, the chemical potential [29, 30]. Therefore, higher order terms in the expansion in powers of the transfer Hamiltonian are non-negligible. In particular, in second order, these lead to an additional non-dissipative contribution $I_1 \cos 2\varphi$ to the coherent flow. It has half of the period $\varphi \rightarrow \varphi + 2\pi$ of the fundamental Josephson current [12] since it is due to the coherent tunneling of two bosonic pairs. Using the results of Ref. [12], the second harmonic current density is linked to the dominant first order term via

$$|j_1| = j_c \frac{|t|(\mu_B)}{4}, \quad (8)$$

which still exhibits the separation between single-particle and many-body properties discussed above for the leading contribution given by Eq. (3).

Moreover, in order to test the predictions of our model against recent experimental data [30] and BEC results of EFTM numerical simulations [46] available in the literature, it is necessary to generalize the results obtained in Eq. (3) to the experimentally relevant case [29, 30] of inhomogeneous samples and Gaussian barriers, see Fig. 1b. In particular, the result in Eq. (3) for the (first order) critical current density can be easily extended to account for an inhomogeneous condensate density profile $n_c(\mathbf{r})$ as

$$\hbar j_c(x, y) = \int_{-R_z}^{R_z} dz n_c(\mathbf{r}) \mu_B(\mathbf{r}) \frac{|t|(\mu_B(\mathbf{r}))}{4 k(\mu_B(\mathbf{r})) R_z} \quad (9)$$

Further integration of j_c along the transverse directions (x, y) then yields the total current

$$\hbar I_c = \int d^3 r n_c(\mathbf{r}) \mu_B(\mathbf{r}) \frac{|t|(\mu_B(\mathbf{r}))}{4 k(\mu_B(\mathbf{r})) R_z}, \quad (10)$$

which obviously recovers the result obtained in the homogeneous case [12], where I_c scales linearly with the junction area A . In the generic inhomogeneous case, Eq. (10) may be regarded as a sum of transmitted particles over all infinitely small volumes centered at position (r, z) , each one containing a number $n_c(r, z)$ of condensed bosons, at energy $\mu_B(r, z)$.

By following a similar procedure and recalling Eq. (8), one can straightforwardly obtain an analytic expression also for the second order contribution to the Josephson current for inhomogeneous samples. While this latter correction is negligible in the deep tunneling limit $V_0/\mu_B \gg 1$, it may cause an up to a 15% increase of the maximum supercurrent I_{Max} in the experimentally relevant regime $V_0/\mu \sim 1$. This can be easily verified on the basis of the analytic results obtained by Goldobin *et al.* [47], that theoretically investigated how an arbitrary second harmonic term in the current-phase relation of a generic junction affects the maximum Josephson current.

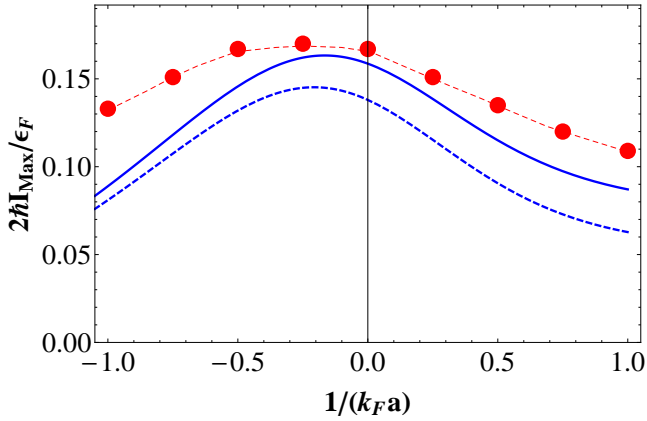


FIG. 3. Critical atom current for a Josephson junction in a box throughout the BEC-BCS crossover. Symbols are the results reported in Ref. [26] for $V_{0f}/\epsilon_F = 5$, $k_F d = 0.6$, $N=100$, $k_F L_\perp = 13$ and $k_F B = 10$. Dashed blue line is the prediction of our model employing the continuum mean field results [41, 44] for μ_B and n_c . Solid blue line is our model prediction accounting for the proper chemical potential of the superfluid in the box geometry [48]. Comparison of the two blue lines highlight the effect of the confining box on the superfluid chemical potential.

III. COMPARISON WITH BdGE NUMERICAL RESULTS FOR THE CROSSOVER REGION

In the following, we compare the predictions of our model for a fixed barrier geometry with numerical results based on the solution of time-dependent mean field BdGE, reported in Ref. [26]. To this end, we consider the specific setup of Zou and Dalfovo [26], analogous to the one sketched in Fig. 1a. In Fig. 3 the dashed line represents the critical fermion current ($2I_{Max}$) predicted by our analytic model for the barrier and reservoir parameters detailed in the figure legend, and employing the mean field continuum results for chemical potential and condensate density, respectively (see Ref. [44] and references therein).

As already emphasized in the previous section, we obtain a non-monotonic critical current as the interaction is changed from the BCS to the BEC regime. Compared with the behavior of $\lambda_0 \sqrt{\mu}$ presented in Fig. 2, the shape of I_{Max} as a function of $1/k_F a$ is quantitatively modified owing to the additional energy dependence of $|t|(\mu_B)$, which monotonically decreases when moving from the BCS towards the BEC limit. In particular, this causes an overall suppression of the maximum Josephson current, more pronounced in the strong attraction limit of tightly bound pairs, where the chemical potential most strongly varies with the coupling strength.

Notably, our model appears in reasonable quantitative agreement with the results of BdGE simulations [26], see red dots in Fig. 3. In particular, the mismatch between our theory and the numerical results is largely ascribable to finite size effects connected with the small box

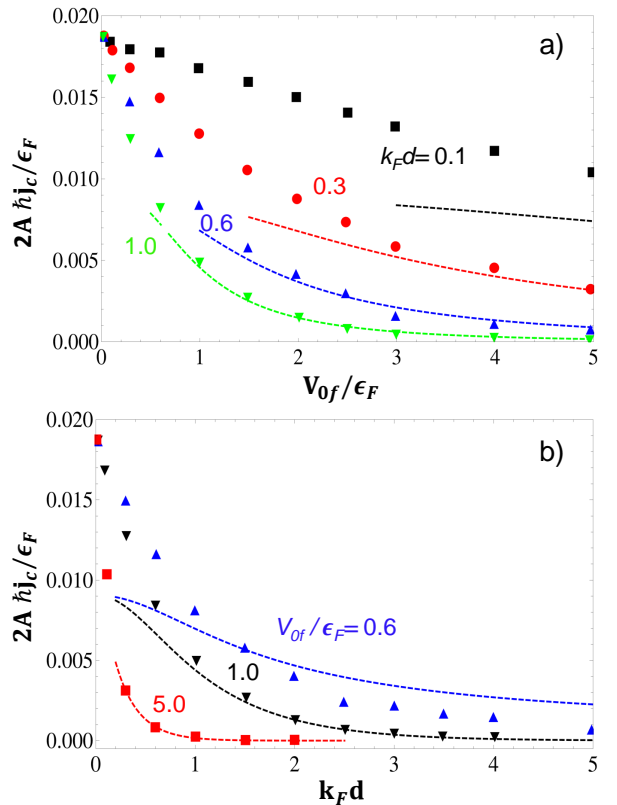


FIG. 4. Critical current density of a unitary superfluid junction in a box geometry and transverse area A . a) Normalized fermion current density $2A\hbar j_c/\epsilon_F$ as a function of barrier height V_{0f}/ϵ_F for different barrier thicknesses, see legend. Symbols are the results reported in Ref. [26]. Lines are the predictions of our analytic model, see Eq. (3), accounting for the proper chemical potential of the gas [48] while assuming the condensed fraction obtained by mean field theory in the continuum [41, 44]. The curves also account for second order contributions, see Eq. (8) and Ref. [47]. b) Same comparison as in panel a) for $2A\hbar j_c/\epsilon_F$ as a function of the barrier thickness and different barrier heights.

employed in the simulation, strongly affecting the bulk superfluid properties, relative to the continuum ones. For instance, the agreement significantly improves when we employ the BdGE chemical potential values obtained within the actual tightly confining box [48], systematically higher than the continuum result, see blue solid line in Fig. 3. In this case, our theory matches the numerical data with deviations not exceeding 30% throughout the crossover region. Additionally, the residual mismatch can be largely attributed to effects not taken into account when evaluating our model predictions: First, the small box size may also cause an increased condensate fraction, relative to the continuum case, especially on the BCS side of the crossover. Second, the determination of the critical current by solving the time dependent BdGE was obtained by imparting a sizable initial excitation to the system [26], yielding an additional kinetic energy contribution to the overall particle energy, neglected in our

model.

The ability of our analytic theory to yield quantitatively accurate Josephson currents in the crossover region is further demonstrated by the comparison presented in Fig. 4. There, we contrast our prediction based on Eq. (3), for the fermion current density ($2\hbar j_c$) of unitary superfluids with the numerical results obtained by Zou and Dalfovo [26] solving stationary BdGE, both as a function of the barrier height for a few values of the dimensionless barrier thickness (Fig. 4a), and vice-versa for different barrier heights as a function of the thickness (Fig. 4b). Following the convention of Ref. [26], the barrier height is given in the legends for one fermion, $V_{0f} = V_0/2$. Apparently, our analytic predictions quantitatively reproduce the numerical results remarkably well over a wide range of barrier geometries. Indeed, as long as the barrier height exceeds the superfluid chemical potential, sizable deviations are observed only for the case of anomalously thin barriers (see black squares in Fig. 4a), for which our theoretical model based on Eq. (3) would converge to the numerical data only for exceedingly high V_0 values. On the other hand and not surprisingly, our model fails even at the qualitative level for $V_0/\mu < 1$, i.e. out of the tunneling regime, see e.g. blue line and triangles in Fig. 4b (BdGE calculations in the present box geometry yield at unitarity $\mu_F/\epsilon_F \sim 0.7$ [48]).

IV. COMPARISON WITH EXPERIMENTS

Finally, we compare our model predictions with experimental data that were obtained in the Lithium lab at LENS [30], and also with EFTM numerical simulations carried out in the BEC limit [46]. To this end, we evaluate the maximum Josephson current I_{Max} accounting for both first and second order contributions [47], in the case of harmonically trapped samples and Gaussian barriers (see Fig. 1b), exploiting Eqs. (10) and (8), respectively. For simplicity, the Gaussian barrier is approximated with an Eckart potential of the form

$$V(z) = \frac{V_0}{\cosh^2(z/d)} \quad (11)$$

for which the single-particle transmission probability can be evaluated analytically, see e.g. Ref. [49]. In particular, it can be verified that a Gaussian profile with e^{-2} waist w can be excellently approximated by an Eckart function with $d \sim 0.6w$. Inserting the transmission amplitude of the Eckart barrier both in Eq. (10) for the first order current and in the analogous expression for the second harmonic based on Eq. (8), and accounting for the relevant superfluid atom number and trap frequencies employed by Burchianti *et al.* [30], we obtain our zero-temperature model predictions for the resulting maximum current I_{Max} [47]. For this comparison, we exploited the chemical potential and condensate fraction obtained within the Luttinger-Ward approach [43]. An important point to emphasize in this context is that the

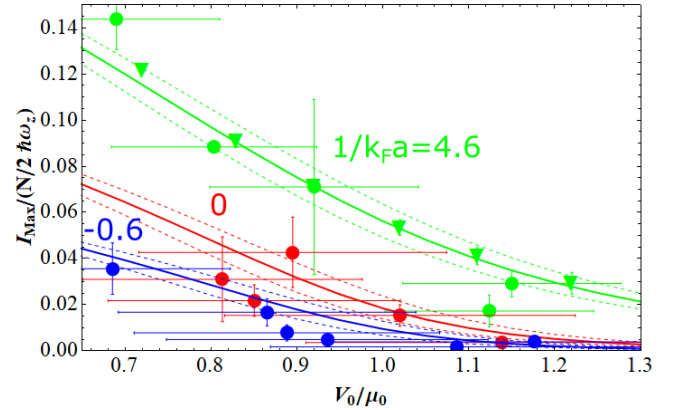


FIG. 5. Critical boson current for trapped superfluids across the BEC-BCS crossover. Experimental data of I_{Max} from Ref. [30], measured as a function of V_0/μ_0 for ${}^6\text{Li}$ fermionic superfluids at unitarity, in the BEC and BCS limit (see legend), are compared with our model predictions (solid lines), employing the μ_B and n_c trends obtained in the Luttinger-Ward approach [43, 51]. In the BEC limit, our results are also compared with EFTM simulations [46] (green triangles). Trap frequencies and atom number were fixed to their mean values in the experiment (nominal value in the simulation). The Gaussian barrier of waist $w \sim 2\mu\text{m}$ employed in the experiment was approximated with an Eckart potential as described in the text. Dashed lines are our model predictions assuming a $\pm 5\%$ variation of the peak chemical potential.

approach provides a quantitatively precise description of the thermodynamic properties not only near unitarity, as shown in Fig. 2, but also in the BCS and the deep BEC limit. Indeed in the regime $1/k_F a > 2$, the normalized chemical potential $\tilde{\mu} \rightarrow k_F a_{dd}/(3\pi)$ approaches the result associated with a dilute gas of Bosons with a dimer-dimer scattering length $a_{dd} = 0.59a$ which is very close to the exact value $a_{dd} = 0.6a$ [50].

The predicted maximum currents $I_{Max}/(N/2 \hbar \omega_z)$ (solid lines) as a function of the barrier height V_0/μ_0 , together with experimental and numerical results (symbols), are summarized in Fig. 5 for BEC (green), crossover (red) and BCS (blue) regimes, respectively. Here μ_0 denotes the pair chemical potential at the center of the cloud evaluated for the superfluid gas in the absence of the repulsive barrier. The different regimes are marked in the legend in terms of the peak interaction parameter $1/k_F a$. We emphasize that, given the relatively small values of V_0/μ_0 accessible in the experiments, second order effects are explicitly included in the evaluation of I_{Max} following Ref. [47]. For each interaction regime, dashed lines represent our model predictions once a $\pm 5\%$ variation of the peak chemical potential is assumed when evaluating the transmission amplitude.

The comparison shown in Fig. 5 clearly demonstrates that our model is able to reproduce the results obtained in the literature so far with remarkable accuracy for all interactions and barrier heights. In particular, we emphasize that our analytic theory quantitatively matches

the ETFM numerical results (green triangles) [46] obtained in the BEC limit even for barrier heights as low as $V_0/\mu_0 \sim 0.7$, i.e. even when a sizable part of the trapped sample is out of the tunneling regime. There, inclusion of second order contributions to I_{Max} is essential, as it yields corrections to the first order term up to 15%. Regarding the crossover and BCS regimes, our model correctly reproduces the observed trends, at least within the large uncertainties of the experimental data and of the zero-temperature approximation done in the theoretical analysis. In particular, we remark that inclusion of the non-perturbative results for both chemical potential and condensate fraction [51] is essential to obtain quantitative agreement with the data, which would not match our theory if mean field results were employed. As a consequence, although more experimental studies are required to fully validate our model within the crossover and BCS regimes, we stress that the measure of the critical Josephson current may provide a valuable experimental tool to determine the condensate density in crossover superfluids, a quantity which is hard to access by other means.

V. CONCLUSIONS AND OUTLOOK

Building on a microscopic model for the Josephson current between two weakly interacting Bose Einstein condensates [12], we have developed a simple theoretical framework which captures the corresponding dynamics of strongly interacting fermionic superfluids throughout the BCS-BEC crossover. As testified by the comparison with available numerical [26, 46] and experimental [30] data, our model provides a quantitative description of the critical currents in generic junction geometries, solely based on bulk properties of the superfluid state and the knowledge of the single boson transmission amplitude. An important feature of our theory is that it provides a consistent explanation for the non-monotonic trend for the maximum Josephson current observed near unitarity. Its origin is connected with the interplay between a decrease of the chemical potential and a concomitant increase of the condensate fraction if the interactions are tuned from the BCS to the BEC limit. By contrast, EFTM models, to which our theory naturally connects deep in the BEC limit, fail for intermediate and weak couplings even at the qualitative level [22, 26] since in these numerical approaches the condensate density coincides by construction with the superfluid one at all couplings. In the future, therefore, it will be interesting to test whether a modified EFTM formalism which explicitly accounts for the reduction of the condensate fraction upon going from the BEC towards the unitary gas and eventually the BCS limit yields results consistent with the ones obtained here or through BdGE approaches. We

also anticipate that our model could be extended to describe dissipative normal currents [30], and to account for finite temperature effects. Moreover, starting from the present study, it might be possible to investigate how the critical current evolves from the tunneling regime considered here to the case of weak barriers studied in Refs. [22, 25, 36].

On a rather fundamental level, it remains an open challenge to justify our use of the result in Eq. (3), which is based on viewing the Josephson effect throughout the BCS-BEC crossover in terms of the coherent tunneling of pairs, by developing a truly microscopic approach which involves the constituent fermions. Within such a description and in the tunneling limit, the Josephson effect is second order in the single fermion tunneling amplitudes t_{kq} . Quite generally, the exact critical current at zero temperature

$$I_c = -\frac{4}{\hbar^2} \sum_{kq} |t_{kq}|^2 \int_0^\infty \frac{d\omega_1}{2\pi} \int_0^\infty \frac{d\omega_2}{2\pi} \frac{B(k, \omega_1)B(q, -\omega_2)}{\omega_1 + \omega_2} \quad (12)$$

can be expressed in terms of the spectral functions $B(k, \omega)$ associated with the anomalous propagator of fermionic superfluids. In the BCS-limit, $B^{\text{BCS}}(k, \omega) = 2\pi u_k v_k [\delta(\omega - E_k/\hbar) - \delta(\omega + E_k/\hbar)]$ is determined by the gap parameter $\Delta_k = u_k v_k 2E_k$ and the excitation energies $E_k = \sqrt{\xi_k^2 + |\Delta_k|^2}$ of the fermionic quasiparticles in the standard manner [52]. The expression Eq. (12) then reduces to the Ambegaokar-Baratoff result Eq. (4) which involves the tunneling probability $|t|^2(\mu_F)$ evaluated right at the Fermi energy. In order to verify within such a fermionic approach the non-monotonic dependence of the critical current on the dimensionless coupling constant $1/k_F a$ along the BCS-BEC crossover, which emerges from our bosonic result Eq. (3), it is required to determine the anomalous spectral functions $B(k, \omega)$ that enter Eq. (12) for arbitrary coupling, a problem which does not seem to have been discussed so far.

ACKNOWLEDGMENTS

We thank F. Dalfovo and P. Zou for providing the chemical potential values relevant to analyze the data of Ref. [26], K. Khani for sharing the ETFM results reported in Ref. [46] for trapped BECs, and B. Frank for the non-perturbative results shown in Fig. 2 and employed to analyze the experimental data of Fig. 4. We acknowledge fruitful discussions with F. Dalfovo, E. Neri, A. Recati, G. Roati, F. Scazza and K. Khani. This work was supported by the ERC through grant no. 637738 PoLiChroM and in part also by the Nano-Initiative Munich (NIM).

-
- [1] B. Josephson, *Physics Letters* **1**, 251 (1962).
- [2] P. W. Anderson and J. M. Rowell, *Phys. Rev. Lett.* **10**, 230 (1963).
- [3] P. Anderson, in *Lectures on the Many-body Problems*, edited by E. Caianiello (Academic Press, 1964) pp. 113 – 135.
- [4] P. W. Anderson, *Rev. Mod. Phys.* **38**, 298 (1966).
- [5] K. K. Likharev, *Rev. Mod. Phys.* **51**, 101 (1979).
- [6] D. J. Van Harlingen, *Rev. Mod. Phys.* **67**, 515 (1995).
- [7] C. C. Tsuei and J. R. Kirtley, *Rev. Mod. Phys.* **72**, 969 (2000).
- [8] J. C. Davis and R. E. Packard, *Rev. Mod. Phys.* **74**, 741 (2002).
- [9] E. Varoquaux, *Rev. Mod. Phys.* **87**, 803 (2015).
- [10] A. Smerzi, S. Fantoni, S. Giovanazzi, and S. R. Shenoy, *Phys. Rev. Lett.* **79**, 4950 (1997).
- [11] I. Zapata, F. Sols, and A. J. Leggett, *Phys. Rev. A* **57**, R28 (1998).
- [12] F. Meier and W. Zwerger, *Phys. Rev. A* **64**, 033610 (2001).
- [13] F. S. Cataliotti, S. Burger, C. Fort, P. Maddaloni, F. Minardi, A. Trombettoni, A. Smerzi, and M. Inguscio, **293**, 843 (2001).
- [14] M. Albiez, R. Gati, J. Fölling, S. Hunsmann, M. Cristiani, and M. K. Oberthaler, *Phys. Rev. Lett.* **95**, 010402 (2005).
- [15] T. Schumm, S. Hofferberth, L. M. Andersson, S. Wildermuth, S. Groth, I. Bar-Joseph, J. Schmiedmayer, and P. Krüger, *Nature Physics* **1**, 57 (2005).
- [16] S. Levy, E. Lahoud, I. Shomroni, and J. Steinhauer, *Nature* **449**, 579 EP (2007).
- [17] L. J. LeBlanc, A. B. Bardou, J. McKeever, M. H. T. Extavour, D. Jervis, J. H. Thywissen, F. Piazza, and A. Smerzi, *Phys. Rev. Lett.* **106**, 025302 (2011).
- [18] F. Jendrzejewski, S. Eckel, N. Murray, C. Lanier, M. Edwards, C. J. Lobb, and G. K. Campbell, *Phys. Rev. Lett.* **113**, 045305 (2014).
- [19] S. Eckel, F. Jendrzejewski, A. Kumar, C. J. Lobb, and G. K. Campbell, *Phys. Rev. X* **4**, 031052 (2014).
- [20] A. Trenkwalder, G. Spagnolli, G. Semeghini, S. Coop, M. Landini, P. Castilho, L. Pezzè, G. Modugno, M. Inguscio, A. Smerzi, and M. Fattori, *Nature Physics* **12**, 826 EP (2016).
- [21] G. Spagnolli, G. Semeghini, L. Masi, G. Ferioli, A. Trenkwalder, S. Coop, M. Landini, L. Pezzè, G. Modugno, M. Inguscio, A. Smerzi, and M. Fattori, *Phys. Rev. Lett.* **118**, 230403 (2017).
- [22] A. Spuntarelli, P. Pieri, and G. C. Strinati, *Phys. Rev. Lett.* **99**, 040401 (2007).
- [23] F. Ancilotto, L. Salasnich, and F. Toigo, *Phys. Rev. A* **79**, 033627 (2009).
- [24] S. K. Adhikari, H. Lu, and H. Pu, *Phys. Rev. A* **80**, 063607 (2009).
- [25] A. Spuntarelli, P. Pieri, and G. Strinati, *Physics Reports* **488**, 111 (2010).
- [26] P. Zou and F. Dalfovo, *Journal of Low Temperature Physics* **177**, 240 (2014).
- [27] D. Stadler, S. Krinner, J. Meineke, J.-P. Brantut, and T. Esslinger, *Nature* **491**, 736 EP (2012).
- [28] D. Husmann, S. Uchino, S. Krinner, M. Lebrat, T. Giamarchi, T. Esslinger, and J.-P. Brantut, *Science* **350**, 1498 (2015).
- [29] G. Valtolina, A. Burchianti, A. Amico, E. Neri, K. Khani, J. A. Seman, A. Trombettoni, A. Smerzi, M. Zaccanti, M. Inguscio, and G. Roati, **350**, 1505 (2015).
- [30] A. Burchianti, F. Scazza, A. Amico, G. Valtolina, J. A. Seman, C. Fort, M. Zaccanti, M. Inguscio, and G. Roati, *Phys. Rev. Lett.* **120**, 025302 (2018).
- [31] W. Zwerger, ed., *The BCS-BEC crossover and the unitary Fermi gas*, Series: Lecture Notes in Physics, Vol. 836 (Springer, Berlin, 2012).
- [32] W. Zwerger, in *Quantum Matter at Ultralow Temperatures*, Vol. 191 of Proceedings of the International School of Physics, edited by M. Inguscio, W. Ketterle, S. Stringari, and G. Roati (IOS Press, Amsterdam) pp. 63 – 142.
- [33] C. Chin, R. Grimm, P. Julienne, and E. Tiesinga, *Rev. Mod. Phys.* **82**, 1225 (2010).
- [34] G. E. Astrakharchik, J. Boronat, J. Casulleras, Giorgini, and S., *Phys. Rev. Lett.* **93**, 200404 (2004).
- [35] R. Combescot, M. Y. Kagan, and S. Stringari, *Phys. Rev. A* **74**, 042717 (2006).
- [36] D. E. Miller, J. K. Chin, C. A. Stan, Y. Liu, W. Setiawan, C. Sanner, and W. Ketterle, *Phys. Rev. Lett.* **99**, 070402 (2007).
- [37] G. Watanabe, F. Dalfovo, F. Piazza, L. P. Pitaevskii, and S. Stringari, *Phys. Rev. A* **80**, 053602 (2009).
- [38] W. Weimer, K. Morgener, V. P. Singh, J. Siegl, K. Hueck, N. Luick, L. Mathey, and H. Moritz, *Phys. Rev. Lett.* **114**, 095301 (2015).
- [39] Formally, $\varphi = \varphi_1 - \varphi_2$ is determined by the phases associated with the anomalous expectation values $\langle \hat{\Psi} \rangle_{1,2} = \sqrt{n_c} e^{i\varphi_{1,2}}$ of the condensates on both sides. It is non-vanishing only in the presence of an externally imposed current $I(\varphi) \neq 0$.
- [40] V. Ambegaokar and A. Baratoff, *Phys. Rev. Lett.* **10**, 486 (1963).
- [41] G. Ortiz and J. Dukelsky, *Phys. Rev. A* **72**, 043611 (2005).
- [42] L. Salasnich, N. Manini, and A. Parola, *Phys. Rev. A* **72**, 023621 (2005).
- [43] R. Haussmann, W. Rantner, S. Cerrito, and W. Zwerger, *Phys. Rev. A* **75**, 023610 (2007).
- [44] S. Giorgini, L. P. Pitaevskii, and S. Stringari, *Rev. Mod. Phys.* **80**, 1215 (2008).
- [45] M. J. H. Ku, A. T. Sommer, L. W. Cheuk, and M. W. Zwierlein, *Science* **335**, 563 (2012).
- [46] K. Khani, E. Neri, L. Galantucci, F. Scazza, A. Burchianti, K. L. Lee, C. F. Barenghi, A. Trombettoni, M. Inguscio, M. Zaccanti, G. Roati, and N. P. Proukakis, “Critical transport and vortex dynamics in a thin atomic Josephson junction,” arXiv:1905.08893.
- [47] E. Goldobin, D. Koelle, R. Kleiner, and A. Buzdin, *Phys. Rev. B* **76**, 224523 (2007).
- [48] P. Zou, Private Communication (2019).
- [49] F. M. Fernández, *American Journal of Physics* **79**, 752 (2011).
- [50] D. S. Petrov, C. Salomon, and G. V. Shlyapnikov, *Phys. Rev. Lett.* **93**, 090404 (2004).
- [51] B. Frank, Private Communication (2019).
- [52] A. L. Fetter and J. D. Walecka, *Quantum Theory of Many-Particle Systems* (McGraw-Hill, Boston, 1971).